

930 **Supplementary Figure 1: HPC projections predominantly target IL neurons in the mPFC.**  
 931 Comparison of hippocampal inputs onto principal neurons in the IL and PL reveal significantly  
 932 larger EPSCs in IL neurons compared to caudal or rostral PL responses (rostral PL:  $n = 12$ ;  
 933 caudal PL:  $n = 5$ ; IL:  $n = 21$  from 7 animals; one-way ANOVA with Dunnett's multiple  
 934 comparison test,  $F_{2,35} = 6.62$ ,  $*P = 0.0037$ ). Dots represent data from individual cells. Error bars  
 935 indicate means  $\pm$  s.e.m.  
 936

937 **Supplementary Figure 2: Hippocampus-driven IL responses are monosynaptic, time-**  
 938 **locked responses.** **a**, Example of a HPC-driven response in a pyramidal neuron, containing the  
 939 initial excitatory response, followed by an inhibitory component. The 5-fold enlarged inset  
 940 shows the time-locked onset of individual responses (grey) to the light stimulation (blue) without  
 941 any response-failures. Averaged response shown in black. Analysis of EPSCs show very low  
 942 response jitter (**b**) (individual jitter of neurons shown as grey dots;  $n = 19$ ) and response latency  
 943 (**c**) ( $n = 14$ ), both typical parameters for monosynaptic responses. Error bars indicate means  $\pm$   
 944 s.e.m.

945 **Supplementary Figure 3: Quantification of vHPC-evoked inhibitory conductances in IL**  
 946 **principal cells.** **a**, Schematic showing experimental setup. Optical terminal stimulation of ventral  
 947 hippocampal inputs and whole-cell recording of pyramidal neurons in the IL. For the spiking  
 948 suppression experiments (**d**), local electrical stimulation (battery symbol) was used. **b**, Current-  
 949 clamp responses to hippocampal terminal release before (black trace) and after (red trace) the  
 950 application of the GABA<sub>B</sub>-receptor antagonist CGP55845 ( $n = 3$ ), revealing the fast (yellow) and  
 951 slow IPSCs (green). **c**, Bar graphs with response patterns of IL principal neurons to optical  
 952 hippocampal stimulation containing fast (top, yellow) and slow (bottom, green) inhibitory  
 953 conductances (percentage of the total). **d**, Investigation of spiking suppression of IL principal  
 954 neurons by the hippocampus. Electrical suprathreshold stimulation was used to evoke spiking  
 955 (left) while presenting optical hippocampal stimulation 150 ms before the spiking event ( $n = 8$ ).  
 956 Blue bars represent optical stimulation.  
 957

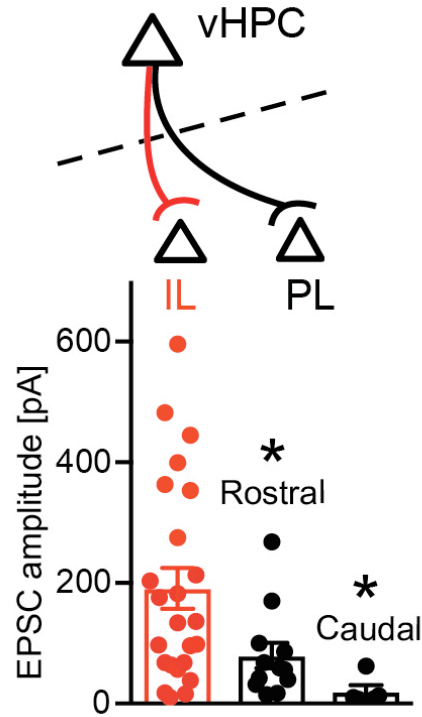
958 **Supplementary Figure 4: Feed-forward inhibition onto pyramidal neurons is mediated by**  
 959 **local IL interneurons.** **a**, Schematic for electrical stimulation (battery symbol) of IL tissue *ex*  
 960 *vivo* in the presence of AMPA- and NMDA-receptor antagonists NBQX and APV, respectively,  
 961 to isolate GABAergic transmission. **b**, Voltage clamp (left) and current-clamp recordings (right)  
 962 revealed inhibitory responses that contain both fast (yellow) and slow (green) inhibitory  
 963 components. **c**, Application of the GABA<sub>B</sub>-receptor antagonist CGP55845 (red trace) isolated the  
 964 fast, inhibitory conductance, which was blocked by the GABA<sub>A/C</sub>-receptor antagonist picrotoxin  
 965 (green trace). Holding voltage: -60 mV.  
 966

967 **Supplementary Figure 5: CNO- and virus-dependent silencing of IL neurons in freely**  
 968 **moving rats.** **a**, Schematic design of experimental approach alongside a representative image  
 969 depicting DREADD-expressing neurons of animals implanted with multichannel recording  
 970 arrays into the IL (40  $\mu$ m coronal section; white bar inset = 250  $\mu$ m). **b**, Vehicle (VEH)  
 971 injections did not cause a significant change in the spontaneous activity (20 s bins) of IL neurons  
 972 ( $n = 15$  for hM4Di;  $n = 27$  for mCherry control) (left). When the hM4D(G<sub>i</sub>)-expressing animal  
 973 was injected with 1 mg/kg (middle) or 3 mg/kg (right) of CNO, IL neurons ( $n = 18$  for 1 mg/kg;  
 974  $n = 16$  for 3 mg/kg) exhibited a significant reduction in spontaneous firing relative to neurons of  
 975 control virus-infected animals ( $n = 25$  for 1 mg/kg;  $n = 23$  for 3 mg/kg; repeated measures

976 ANOVA, main effects of virus:  $F_{1,41} = 10.912$ ,  $**P = 0.0020$  for 1 mg/kg;  $F_{1,37} = 24.375$ ,  $***P <$   
977  $0.0001$  for 3 mg/kg).  
978

**Supplementary Figure 6: Pharmacological inactivation of the IL impedes retrieval of extinguished fear.** Test data show mean baseline freezing (3 min), mean freezing during nine 5-ITI blocks (30-sec ITIs) and a during a post-trial period (150 sec) following infusions of muscimol or vehicle into the IL (MUSC,  $n = 6$ ; VEH,  $n = 10$ ; repeated measures ANOVA, main effect of drug:  $F_{1,14} = 35.78$ ,  $***P < 0.0001$ ). Corresponding conditioning and extinction data are shown in Fig. 4. Error bars indicate means  $\pm$  s.e.m.

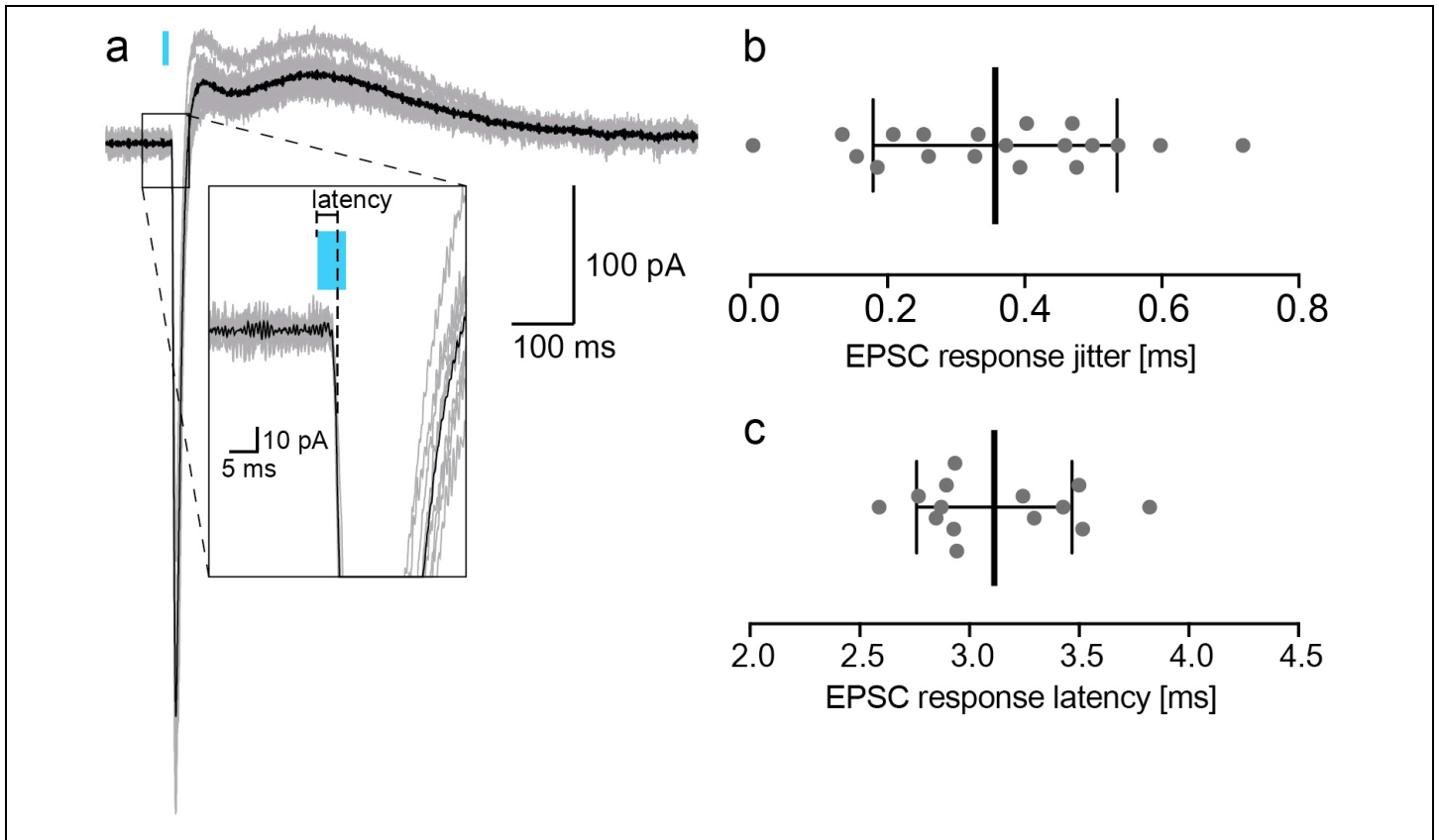
979



Supplementary Figure 1

**HPC projections predominantly target IL neurons in the mPFC.**

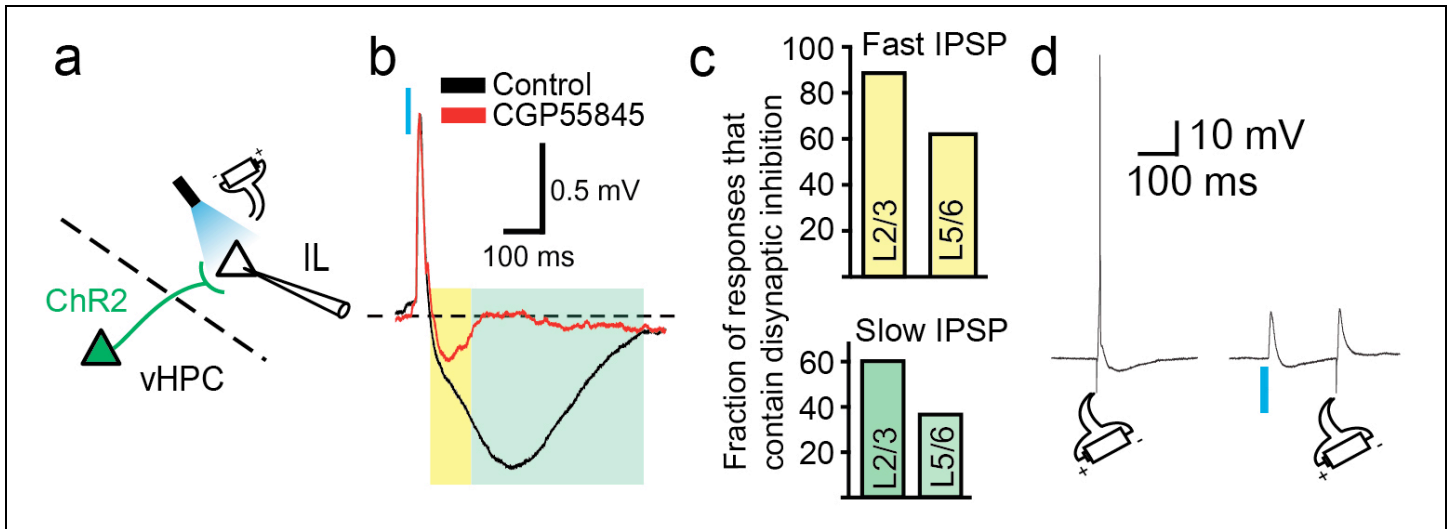
Comparison of hippocampal inputs onto principal neurons in the IL and PL reveal significantly larger EPSCs in IL neurons compared to caudal or rostral PL responses (rostral PL:  $n = 12$ ; caudal PL:  $n = 5$ ; IL:  $n = 21$  from 7 animals; one-way ANOVA with Dunnett's multiple comparison test,  $F_{2,35} = 6.62$ ,  $*P = 0.0037$ ). Dots represent data from individual cells. Error bars indicate means  $\pm$  s.e.m.



**Supplementary Figure 2**

**Hippocampus-driven IL responses are monosynaptic, time-locked responses.**

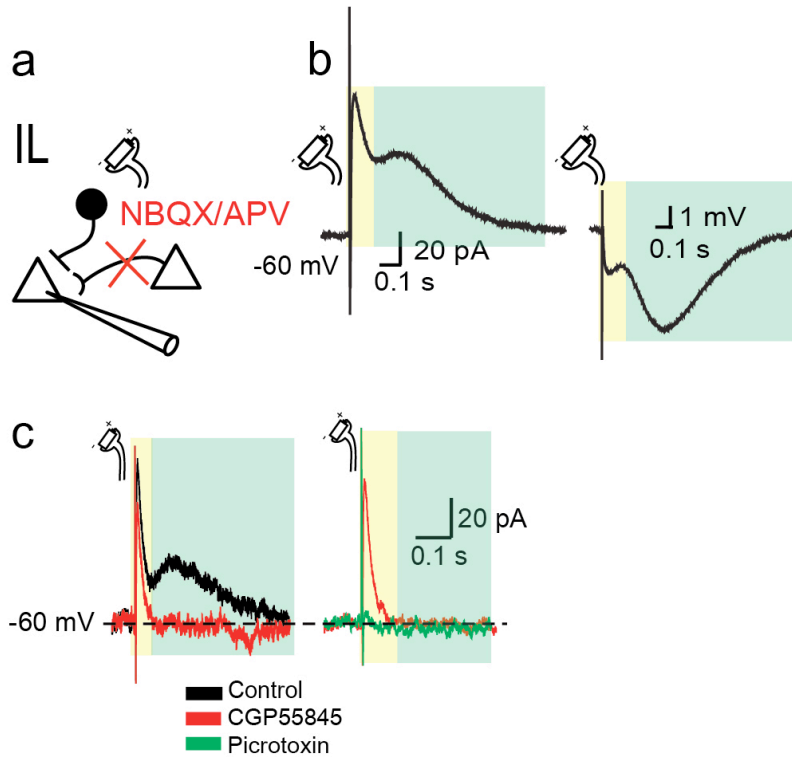
**a**, Example of a HPC-driven response in a pyramidal neuron, containing the initial excitatory response, followed by an inhibitory component. The 5-fold enlarged inset shows the time-locked onset of individual responses (grey) to the light stimulation (blue) without any response-failures. Averaged response shown in black. Analysis of EPSCs show very low response jitter (**b**) (individual jitter of neurons shown as grey dots;  $n = 19$ ) and response latency (**c**) ( $n = 14$ ), both typical parameters for monosynaptic responses. Error bars indicate means  $\pm$  s.e.m.



### Supplementary Figure 3

#### Quantification of vHPC-evoked inhibitory conductances in IL principal cells.

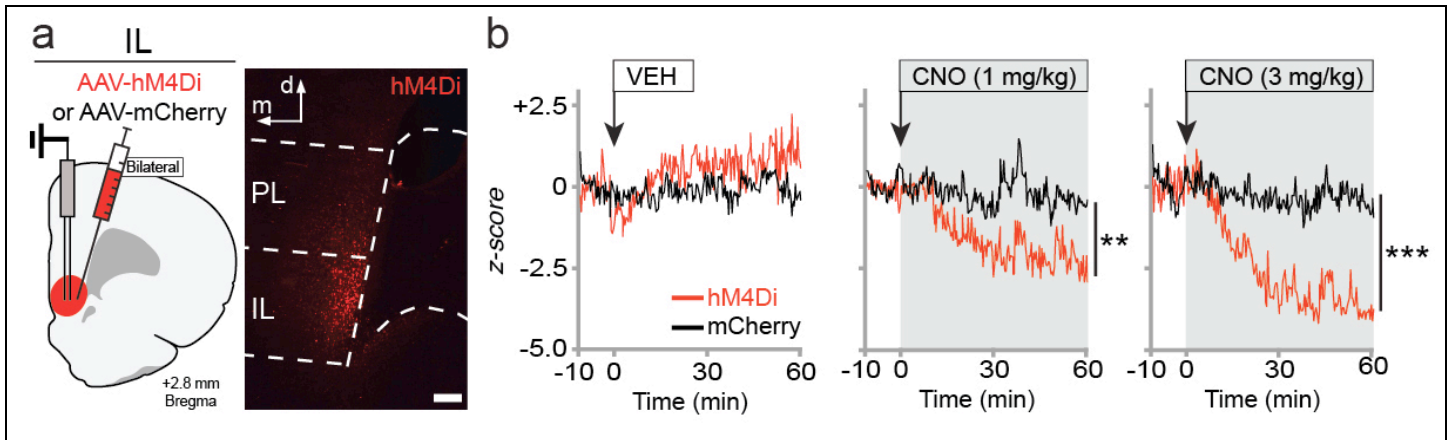
**a**, Schematic showing experimental setup. Optical terminal stimulation of ventral hippocampal inputs and whole-cell recording of pyramidal neurons in the IL. For the spiking suppression experiments (**d**), local electrical stimulation (battery symbol) was used. **b**, Current-clamp responses to hippocampal terminal release before (black trace) and after (red trace) the application of the GABA<sub>B</sub>-receptor antagonist CGP55845 ( $n = 3$ ), revealing the fast (yellow) and slow IPSCs (green). **c**, Bar graphs with response patterns of IL principal neurons to optical hippocampal stimulation containing fast (top, yellow) and slow (bottom, green) inhibitory conductances (percentage of the total). **d**, Investigation of spiking suppression of IL principal neurons by the hippocampus. Electrical suprathreshold stimulation was used to evoke spiking (left) while presenting optical hippocampal stimulation 150 ms before the spiking event ( $n = 8$ ). Blue bars represent optical stimulation.



**Supplementary Figure 4**

**Feed-forward inhibition onto pyramidal neurons is mediated by local IL interneurons.**

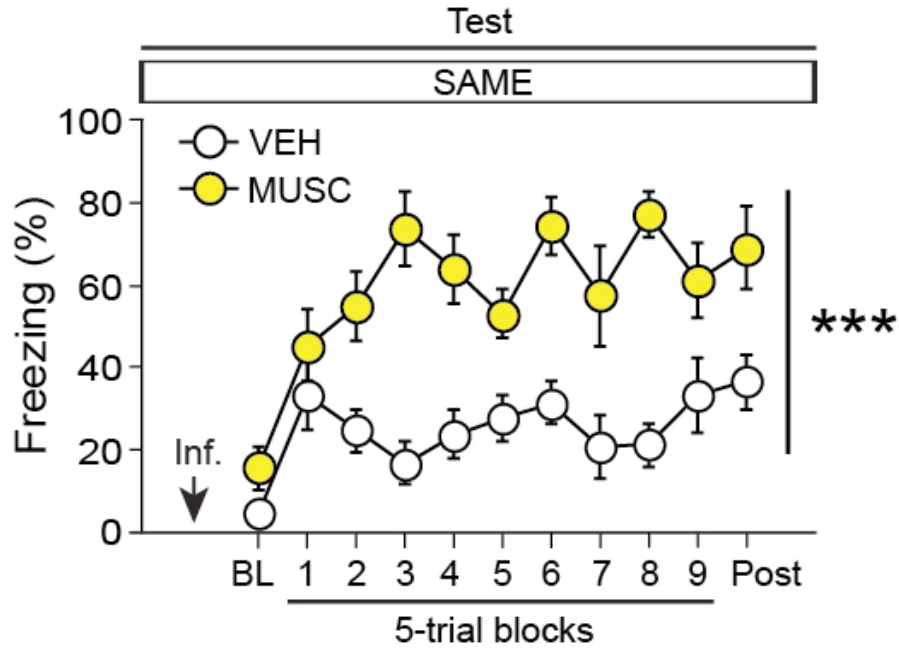
**a**, Schematic for electrical stimulation (battery symbol) of IL tissue *ex vivo* in the presence of AMPA- and NMDA-receptor antagonists NBQX and APV, respectively, to isolate GABAergic transmission. **b**, Voltage clamp (left) and current-clamp recordings (right) revealed inhibitory responses that contain both fast (yellow) and slow (green) inhibitory components. **c**, Application of the GABA<sub>B</sub>-receptor antagonist CGP55845 (red trace) isolated the fast, inhibitory conductance, which was blocked by the GABA<sub>A/C</sub>-receptor antagonist picrotoxin (green trace). Holding voltage: -60 mV.



**Supplementary Figure 5**

**CNO- and virus-dependent silencing of IL neurons in freely moving rats.**

**a**, Schematic design of experimental approach alongside a representative image depicting DREADD-expressing neurons of animals implanted with multichannel recording arrays into the IL (40  $\mu\text{m}$  coronal section; white bar inset = 250  $\mu\text{m}$ ). **b**, Vehicle (VEH) injections did not cause a significant change in the spontaneous activity (20 s bins) of IL neurons ( $n = 15$  for hM4Di;  $n = 27$  for mCherry control) (left). When the hM4D(G<sub>i</sub>)-expressing animal was injected with 1 mg/kg (middle) or 3 mg/kg (right) of CNO, IL neurons ( $n = 18$  for 1 mg/kg;  $n = 16$  for 3 mg/kg) exhibited a significant reduction in spontaneous firing relative to neurons of control virus-infected animals ( $n = 25$  for 1 mg/kg;  $n = 23$  for 3 mg/kg; repeated measures ANOVA, main effects of virus:  $F_{1,41} = 10.912$ ,  $**P = 0.0020$  for 1 mg/kg;  $F_{1,37} = 24.375$ ,  $***P < 0.0001$  for 3 mg/kg).



**Supplementary Figure 6**

**Pharmacological inactivation of the IL impedes retrieval of extinguished fear.**

Test data show mean baseline freezing (3 min), mean freezing during nine 5-ITI blocks (30-sec ITIs) and a during a post-trial period (150 sec) following infusions of muscimol or vehicle into the IL (MUSC,  $n = 6$ ; VEH,  $n = 10$ ; repeated measures ANOVA, main effect of drug:  $F_{1,14} = 35.78$ ,  $***P < 0.0001$ ). Corresponding conditioning and extinction data are shown in Fig. 4. Error bars indicate means  $\pm$  s.e.m.